J. Synchrotron Rad. (1998). **5**, 67–71

Experimental Characterization of APS Undulator A at High Photon Energies (50–200 keV)

S. D. Shastri,* R. J. Dejus and D. R. Haeffner

Advanced Photon Source, Argonne National Laboratory, Argonne, IL 60439, USA. E-mail: shastri@aps.anl.gov

(*Received 8 July 1997; accepted 15 October 1997*)

The considerable intensity of Advanced Photon Source (APS) undulator A as a source of high-energy X-rays permits the performance of numerous types of experiments that require such photon energies. Measured and calculated properties, in the 50–200 keV range, of the X-ray beam from undulator A, installed in sector 1 of the APS, are presented. The flux spectra observed at various gaps agree well with calculations that incorporate the actual magnetic field within the device and the emittance and energy spread of the stored positrons. The field errors and energy spread cause the X-ray beam to lose undulator radiation properties at high energies, as seen in the smeared-out spectral harmonics and increased beam divergence, giving resemblance to a low-K wiggler source. Owing to the wiggler-like behavior in this photon-energy range, the optimal operating condition for undulator A is in the vicinity of the closed-gap setting, corresponding to a maximum critical energy.

Keywords: undulators; insertion devices; X-ray sources; high-energy X-rays.

1. Introduction

The salient physical properties of the interaction between high-energy X-rays (>50 keV) and matter include low attenuation, almost extinction-free (*i.e.* kinematical) diffraction, small scattering angles, accessibility of large momentum transfers, and the absence of anomalous scattering when working with medium to lightweight element samples. These features, in various combinations, benefit certain types of experiments (Freund, 1988; Schneider, 1995). Long penetration lengths aid studies of crystal quality (Schneider *et al.*, 1989), material bulk properties (Neumann *et al.*, 1995), phenomena related to weak scattering mechanisms (*e.g.* nonresonant magnetic scattering; Strempfer *et al.*, 1996) and samples (*e.g.* amorphous matter; Badyal *et al.*, 1997) in thick-walled containment. The absence of extinction and anomalous scattering simplifies the analysis of diffraction data, as can small scattering angles by mitigating the uncertainty of polarization corrections. Compton scattering studies (Blaas *et al.*, 1995) are assisted by the improved validity of the impulse approximation and the enhancement of the Compton cross section relative to the photoelectric cross section. The availability of intense high-energy synchrotron X-rays also permits the exploitation of anomalous-scattering techniques with heavy elements and the possibility of exciting additional nuclear resonances.

Motivated by the scientific possibilities listed above, an earlier paper (Shastri *et al.*, 1996) was written that presented calculated results predicting the high-energy performance of two types of insertion devices available at the Advanced Photon Source (APS): undulator A and wiggler A. A conclusion drawn there was that undulator A should perform better than wiggler A for most experiments up to at least ~280 keV, a range likely to encompass the majority of high-energy experiments to be pursued in the near future. The recent commencement of operation of the APS storage ring offered the opportunity to characterize experimentally the performance of undulator A, the primary insertion device of interest. Low-energy-regime (<50 keV) diagnostics of undulator A, along with emittance measurement methods, are described elsewhere (Cai *et al.*, 1996). The present paper describes the measured performance of undulator A at 50–200 keV, a pho-

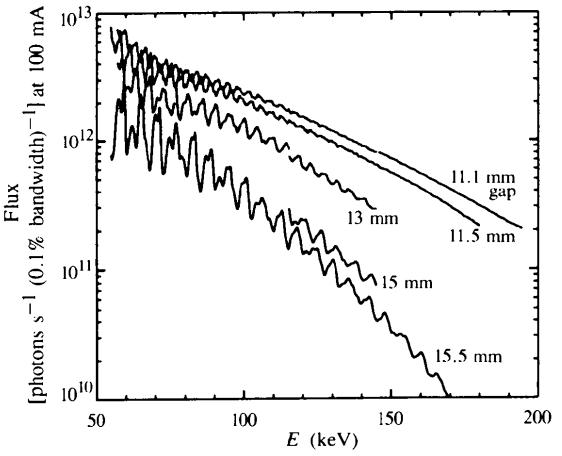

Figure 1
UA flux spectra for five gaps corresponding to deflection-parameter values K = 2.570, 2.464, 2.108, 1.718 and 1.633. These spectra were measured through a 1 × 1 mm^2 aperture positioned on-axis, 35 m from the source.

ton-energy range in which the undulator radiation properties are strongly affected by both field errors and, to a lesser extent, the particle-beam energy spread. All measurements were made on the insertion device designated UA#7, installed in the sector 1 straight section of the 7 GeV APS storage ring. Like all other standard undulators A, UA#7 is a 3.3 cm-period permanent-magnet device with 72 periods (Lai *et al.*, 1993; Dejus *et al.*, 1994). In the dispersionless straight section, during the time of measurements, the positron beam had phase-space parameters $(\sigma_x, \sigma_{x'}, \sigma_y, \sigma_{y'}) = (330\ \mu m, 23\ \mu rad, 70\ \mu m, 7.0\ \mu rad)$ and a relative energy spread $\sigma_E/E = 0.1\%$. The comparisons between calculations and measurements in the next section are mostly sensitive to σ_E/E, $\sigma_{x'}$ and $\sigma_{y'}$. The value for σ_E/E was based on the storage-ring parameters, and the values for $\sigma_{x'}$ and $\sigma_{y'}$ were obtained from fitting the beam profile at a low-order harmonic.

2. Spectral flux

Fig. 1 shows measured flux spectra through a $1 \times 1\ mm^2$ aperture placed 35 m from UA#7 for five undulator gaps. These were obtained by passing the apertured undulator white beam through filters to reduce the heat load on a monochromator, which consisted of an internally water-cooled symmetrically cut perfect Si(111) crystal that was scanned in angle to record the undulator radiation spectrum. The horizontally diffracted monochromatic beam was detected by an N_2-gas-filled ionization chamber. The recorded signal was corrected for detector efficiency, filter attenuation, storage-ring current decay and intrinsic bandpass of the crystal reflection to obtain the final plotted quantity: photons s^{-1} (0.1% bandwidth)$^{-1}$ at 100 mA. The choice of a single-bounce geometry is desirable for an absolute flux measurement because, for a stationary crystal in a white beam, the diffracted flux is insensitive to moderate lattice distortions caused by heat load, fabrication or mounting. So, for the intrinsic bandpass of the reflection, one can still use the value calculated from dynamical diffraction theory. In contrast, the flux after a double-reflection setup is well known to depend sensitively on the slightest distortions in either of the two crystals.

The five spectra in Fig. 1 exhibit smearing of high-energy spectral features to different degrees. The effect is most apparent at small gaps, indicating that the extent of influence of field errors depends more directly on spectral harmonic number than on photon energy. This is sensible because, for example, the effective phase error governing the degradation of the nth harmonic is $n\sigma_\varphi$, where σ_φ is the r.m.s. phase error of the undulator. For UA#7, $\sigma_\varphi < 5°$ at all gaps.

The manner in which the curves in Fig. 1 branch away from one another, without overlap, clearly reveals that operating close to the smallest possible gap is the best configuration for experiments utilizing photons of energy above 50 keV. This is in marked distinction from the case of operating below 50 keV, where the spectra for different gaps overlap in a complicated fashion, requiring examination of undulator tuning curves for aid in the selection of the optimum gap or harmonic (Lai *et al.*, 1993; Dejus *et al.*, 1994).

Magnetic field profiles were obtained for the undulator at the APS magnet measurement facility (Burkel *et al.*, 1993). Those profiles were taken for a set of gaps that coincide with our choice of spectral measurement gaps at two values, 15.5 and 11.5 mm. For these two cases the computer code *UR* (undulator radiation; Dejus & Luccio, 1994) was run to calculate the expected flux, taking into account the measured magnetic field, emittance and particle-beam energy spread. Figs. 2 and 3 show the comparison between calculation and experiment. The fine jaggedness in the calculated curves is a computational effect due to the Monte Carlo treatment of the storage-ring emittance. At a 15.5 mm gap (Fig. 2), the agreement is good, not only in terms of the overall absolute flux but in the substructure of the harmonics. The same holds for the 11.5 mm gap comparison (Fig. 3) up to about 100 keV, after which there is a gradually increasing flux discrepancy

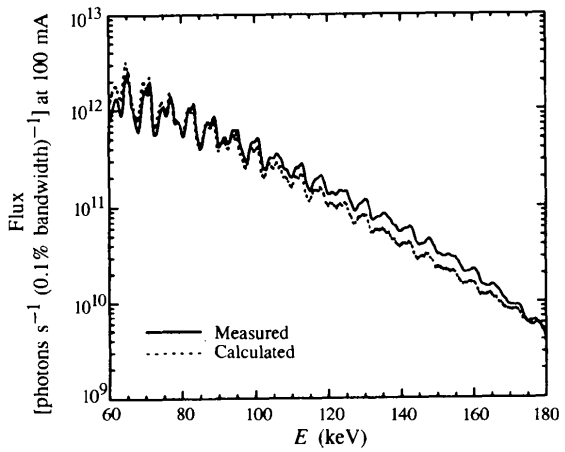

Figure 2
Comparison of measured and calculated spectra for a 15.5 mm gap (K = 1.633).

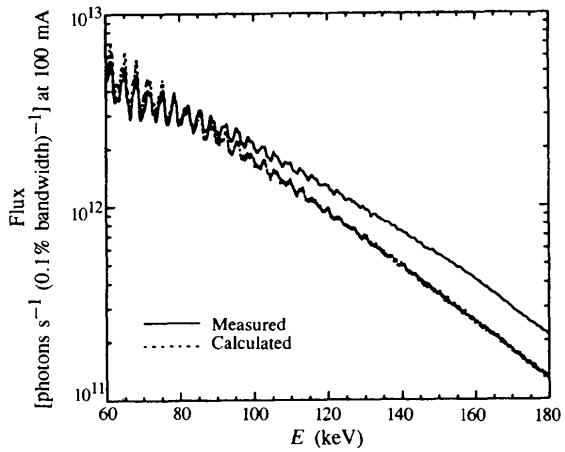

Figure 3
Comparison of measured and calculated spectra for an 11.5 mm gap (K = 2.464).

that grows to slightly under a factor of two at 180 keV, the measured quantity being larger.

The flux disagreement towards the high end of the energy range for the 11.5 mm gap is because of the increased heat load on the Si crystal due to the small gap. Earlier in this section the claim was made that single-crystal reflection geometry is relatively forgiving for absolute flux measurements even when thermal strains are present in the lattice. This is true provided the strain length scale is larger than the so-called extinction length of the Bragg reflection. Here, strain length scale refers to the distance over which the curvature of the lattice in angle is comparable with the angular Darwin width of the reflection. In extreme cases of high heat loads and/or very small Darwin widths, the condition just mentioned ceases to hold and the crystal will diffract partly kinematically, instead of fully dynamically, generally giving more reflected flux. In the 100–200 keV range the Si(111) Darwin width becomes a small fraction of an arcsecond, making it likely that under small-gap conditions of APS undulator A, even with power filtering, thermal distortion becomes significant.

3. Beam divergence

Just as the undulator property of well defined spectral harmonics is suppressed at high energies by field errors and particle energy spread, so should be the characteristic of a collimated central cone of radiation. (Also, for the high-order harmonics, the closely spaced satellite rings around the central cone give rise to more-pronounced profile tails because of broadening by the particle-beam emittance.) At high energies, for an imperfect device, the central cone dominated by emittance should give way to a less collimated beam with vertical and horizontal divergences roughly of order $1/\gamma$ and K/γ, respectively, as expected from wiggler behavior. Here, γ is the relativistic parameter of the particles defined as the ratio of total energy to rest energy, and K is the deflection parameter associated with the insertion device.

To examine the beam divergence effect in the vertical direction an aperture much smaller than the beam size was positioned upstream of the monochromator and scanned vertically through the center of the beam 35 m from the source. This was done at numerous photon energies for two undulator gaps, 15.5 and 11.5 mm. The full width at half maximum (FWHM) beam sizes from the profiles are summarized in Figs. 4 and 5, after having converted them to angular divergences. Two symbol types distinguish FWHMs taken in spectral 'valleys' from those taken on spectral peaks, such as on harmonics or secondary peaks that often accompany harmonics on the low-energy side. The solid line in both figures represents wiggler behavior for the on-axis ($\theta = 0$) vertical divergence and is given by (Kim, 1989)

$$\mathrm{FWHM} = \frac{4}{\gamma}\left(\frac{\pi \ln 2}{3}\right)^{1/2} \frac{\int_y^\infty K_{5/3}(\xi)\, d\xi}{y K_{2/3}^2(y/2)}, \qquad (1)$$

where $y = E/\{E_c[1 - (\theta\gamma/K)^2]^{1/2}\}$. Here, E is the photon energy and E_c is the on-axis critical energy that is related to the peak magnetic field, and hence K. The functions $K_{5/3}$ and $K_{2/3}$ are fractional-order modified Bessel functions of the second kind. In the case of the 15.5 mm gap (Fig. 4), beam divergences measured at energies corresponding to spectral peaks are smaller than those measured in valleys, showing that collimation and spectral enhancement are concomitant manifestations of an undulator's interference effect at certain energies. Furthermore, the asymptotic clustering of points close to the wiggler curve towards high energies is evident. Similar comments can be made with regard to the 11.5 mm gap results (Fig. 5), with the additional observation that convergence towards the wiggler curve occurs at lower energy. This is consistent with the

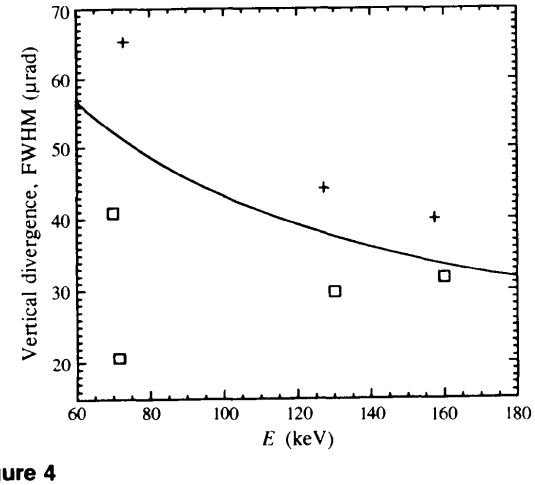

Figure 4
Vertical beam divergences for a 15.5 mm gap (K = 1.633). Two point symbols differentiate measurements made on spectral peaks (squares) from those made in valleys (+). The solid line is calculated from the wiggler expression (1) in the text, using a critical energy E_c = 17.3 keV.

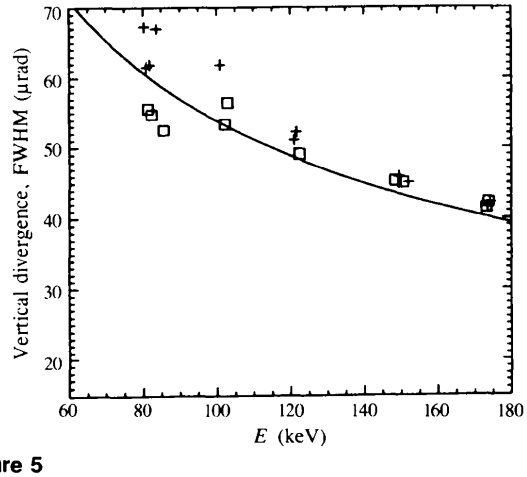

Figure 5
Vertical beam divergences for an 11.5 mm gap (K = 2.464). Two point symbols differentiate measurements made on spectral peaks (squares) from those made in valleys (+). The solid line is calculated from the wiggler expression (1) in the text, using a critical energy E_c = 26.1 keV.

statement made in the preceding section that the impact of field errors is directly related to harmonic number rather than energy, thereby affecting the undulator radiation properties at lower energies when the gap is reduced.

At the time of these measurements a fixed aperture in the beamline prevented determinations of the full horizontal divergence at high energies. However, assuming a wiggler treatment to be valid at high energies, one should expect the horizontal profile of the beam along the orbital plane to be proportional to (Kim, 1989)

$$y^{3/2} \int_y^\infty K_{5/3}(\xi)\, d\xi. \qquad (2)$$

The dependence on the horizontal observation angle θ occurs through the quantity y defined earlier. As an example, using a gap of 11.5 mm and E = 80 keV as the photon energy of interest, evaluation of expression (2) gives a horizontal profile whose FWHM $\simeq 1.3K/\gamma \simeq$ 230 μrad, which is significantly larger than the vertical divergences shown in Fig. 5. At a distance of 35 m, this beam will have a spatial size of 8 × 2 mm^2 FWHM.

4. Concluding remarks

The APS undulators have been magnetically tuned to ensure high brilliance of the low-order harmonics (up to the seventh harmonic) and to minimize perturbation of the stored particle beam. It is well known that the high-order harmonics depend more sensitively on the magnetic field quality of the device and the storage-ring beam parameters than the low-order ones. Calculations indicate (Moog *et al.*, 1997) that the on-axis brilliance will be already smeared out by the 25th harmonic (above 80 keV) at a gap of 11.5 mm using a device with relatively large magnetic field errors (r.m.s. phase error of 4.6°). For the undulator UA#7 used here, with an r.m.s. phase error of 3.2° at an 11.5 mm gap, the harmonics are clearly usable well beyond 80 keV, as can be seen in Fig. 1, which is a manifestation of the quality of the insertion devices currently at third-generation synchrotron radiation facilities.

The combination of magnetic field errors and particle-beam energy spread has a dramatic effect on the high-order harmonics and can amount to a tenfold reduction of intensity in comparison with an ideal device and no beam energy spread. For the purpose of utilizing high-order harmonics, the spectral shimming adjustment of insertion devices should be pursued further to reduce the r.m.s. phase error below 2.5° (the smallest value, at present, for undulator A device types), and efforts to minimize the particle-beam energy spread would also be desirable. However, even under conditions where undulator radiation behavior is diminished or absent, one should note that undulator A beam characteristics become those of a low-K wiggler, whose horizontal collimation is significantly better than that of conventional wigglers with large K.

When operating at small gaps, the performance of APS undulator A makes it an intense source of high-energy X-rays. [A comparison of APS undulator A and wiggler A with sources in other synchrotron facilities can be found in the article by Shastri *et al.* (1996).] With the smallest currently allowable gap of 11.1 mm and a 1 × 1 mm^2 aperture placed 35 m from the source, a perfect-crystal Si(111) monochromator, corresponding to an integrated reflectivity bandpass of 1.7 × 10^{-4}, produces 10^{12}–10^{11} photons s^{-1} in the 50–150 keV range. If a particular experiment permits the use of an imperfect- or bent-crystal monochromator of larger integrated reflectivity, a flux improvement of another order of magnitude can result. Furthermore, because the particle-beam energy spread and field errors inherent in the actual device result in a beam whose size at 35 m is much greater than 1 × 1 mm^2, focusing optics can increase the flux on a millimeter-sized sample beyond 10^{13} photons s^{-1} at around 100 keV, thereby exploiting the full potential of undulator A.

The assistance of M. Keeffe, G. Srajer, J. Lang and C. Nelson during measurements, and discussions with D. Mills and E. Gluskin are gratefully acknowledged. This work is supported by the US Department of Energy, BES-Materials Sciences, under contract No. W-31-109-ENG-38.

References

Badyal, Y. S., Saboungi, M.-L., Price, D. L., Haeffner, D. R. & Shastri, S. D. (1997). *Europhys. Lett.* **39**, 19–24.

Blaas, C., Redinger, J., Manninen, S., Honkimäki, V., Hämäläinen, K. & Suortti, P. (1995). *Phys. Rev. Lett.* **75**, 1984–1987.

Burkel, L., Dejus, R., Maines, J., O'Brien, J., Pfluger, J. & Vasserman, I. (1993). Report ANL/APS/TB-12. Argonne National Laboratory, IL 60439, USA.

Cai, Z., Dejus, R. J., Den Hartog, P., Feng, Y., Gluskin, E., Haeffner, D., Illinski, P., Lai, B., Legnini, D., Moog, E. R., Shastri, S., Trakhtenberg, E., Vasserman, I. & Yun, W. (1996). *Rev. Sci. Instrum.* **67**(9), CD ROM.

Dejus, R. J., Lai, B., Moog, E. R. & Gluskin, E. (1994). Report ANL/APS/TB-17. Argonne National Laboratory, IL 60439, USA.

Dejus, R. J. & Luccio, A. (1994). *Nucl. Instrum. Methods*, A**347**, 61–66.

Freund, A. K. (1988). Editor. *Workshop on Applications of High-Energy X-ray Scattering*. ESRF, Grenoble, France.

Kim, K.-J. (1989). *AIP Conference Proceedings 184*, Vol. 1, *Physics of Particle Accelerators*, edited by M. Month & M. Dienes, pp. 565–633. New York: American Institute of Physics.

Lai, B., Khounsary, A., Savoy, R., Moog, E. & Gluskin, E. (1993). Report ANL/APS/TB-3. Argonne National Laboratory, IL 60439, USA.

Moog, E. R., Vasserman, I., Borland, M., Dejus, R., Den Hartog, P. K., Gluskin, E., Maines, J. & Trakhtenberg, E. (1997). *Magnetic Performance of Insertion Devices at the Advanced Photon Source, 1997 Particle Accelerator Conference Proceedings*, Vancouver, BC, Canada. In the press.

Neumann, H.-B., Rütt, U., Schneider, J. R. & Shirane, G. (1995). *Phys. Rev. B*, **52**, 3981–3984.

Schneider, J. R. (1995). Editor. *International Workshop on Scattering Experiments with High-Energy Synchrotron Radiation*. HASYLAB/DESY, Hamburg, Germany.

Schneider, J. R., Nagasawa, H., Berman, L. E., Hastings, J. B., Siddons, D. P. & Zulehner, W. (1989). *Nucl. Instrum. Methods*, A**276**, 636–642.

Shastri, S. D., Dejus, R. J., Haeffner, D. R. & Lang, J. C. (1996). *Rev. Sci. Instrum.* **67**(9), CD ROM.

Strempfer, J., Brückel, T., Rütt, U., Schneider, J. R., Liss, K.-D. & Tschentscher, T. (1996). *Acta Cryst.* A**52**, 438–449.